JOURNAL OF Materials CHEMISTRY

The effect of molecular shape on the liquid crystal properties of the mono-*O*-(2-hydroxydodecyl)sucroses†

Yves Queneau,[a] Juliette Gagnaire,[a] Jon J West,[b] Grahame Mackenzie[c] and John W Goodby[b]

[a]*Laboratoire de Sucrochimie, UMR 143 CNRS, c/o Béghin-Say, CEI, BP 2132, 27 bd du 11 Novembre 1918, 69603 Villeurbanne, Cedex, France*
[b]*The Liquid Crystals and Advanced Materials Centre, Department of Chemistry, The University of Hull, Hull, UK HU6 7RX*
[c]*The Lipids Research Centre, Department of Chemistry, The University of Hull, Hull, UK HU6 7RX*

Received 11th June 2001, Accepted 6th August 2001
First published as an Advance Article on the web 8th October 2001

In this study we have varied the position of attachment of an aliphatic chain to a disaccharide sucrose unit, and we have shown that the point of attachment can markedly influence the self-organising properties and structure and bonding features of the material. The location of the attachment can introduce curvature into the system thereby stabilising certain structures over others. The results obtained for the thermotropic liquid crystalline properties of the mono-*O*-(2-hydroxydodecyl)sucroses show a similar dependency on molecular shape and curvature as those found in general for lyotropic systems.

1. Introduction

In classical non-carbohydrate and non-amphiphilic thermotropic liquid crystal systems, it is common to develop property–structure correlations *via* the investigation of the variation in transition temperature(s) as a function of systematic changes in molecular structure.[1] Usually, it is found that the clearing and mesophase to mesophase transition temperatures are extremely sensitive to small structural changes at the molecular level, and, in fact, many studies have been made in relation to the effects of substituent size and position on mesomorphic properties. Conversely, similar studies for amphotropic systems with respect to their thermotropic and/or their lyotropic behaviours are less well developed.[2] However, one such comparison has been completed for the thermotropic properties of the *x*-*O*-dodecyl-α,β-D-glucopyranoses by Miethchen and other researchers.[3] Miethchen *et al.* demonstrated the effect on clearing point temperatures as a dodecyl chain is moved sequentially from one position to the next in substituted D-glucopyranose systems, see Fig. 1.

In Fig. 1, the dodecyl chain is moved from the 1- to the 6-position, however, the ratio of α to β anomer for this series of materials varies from one member to the next, except for the 1-*O*-substituted homologue where either 100% α or 100% β anomer is present. Nevertheless, even though the anomeric purity varies across the series, the clearing points range from 140 to 167.2 °C, with the 2-substituted compound having the highest clearing temperature and the 4-substituted compound the lowest. Interestingly, the mesophase exhibited by all of the homologues is the same; *i.e.* a smectic A_d* phase. The fact that the mesophase type is lamellar suggests the shapes of the molecules, for each of the members of the series, are rod-like, with the carbohydrate head group having a similar cross-sectional area to the aliphatic chain. As a consequence, the sequential movement of the chain does not engender any curvature into the system which might lead to the formation of cubic or columnar phases.

In order to extend these studies further we decided to examine the effect on mesomorphic properties of the position of substitution of an aliphatic chain in disaccharide systems. By introducing a disaccharide unit we expected that the relative cross-sectional area of the sugar head group would vary considerably as the aliphatic chain was moved sequentially from one position to the next.

Although the family of mesogenic glycolipids, which have molecular architectures composed of either pyranose, furanose, or acyclic monosaccharide units and a single alkyl chain, is growing, the number of mesogenic glycolipids that have head groups that possess two or more sugar units bonded to each other in a linear or branched fashion remains relatively small. For example, most mesogenic disaccharide compounds synthesised have been derived from reducing disaccharides

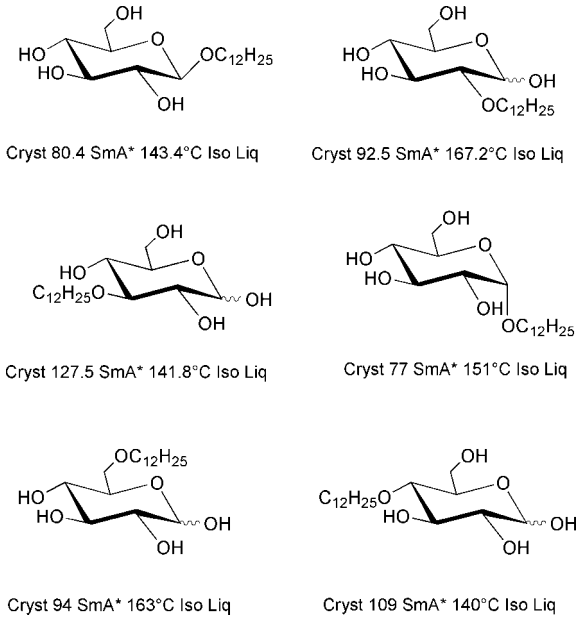

Fig. 1 Mesophase transition temperatures as a function of position of the chain in dodecyl substituted glucopyranosides.[3]

†Basis of a presentation given at Materials Discussion No. 4, 11–14 September 2001, Grasmere, UK.

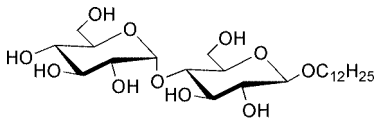

1 Cr 80 SmA 244°C Iso Liq

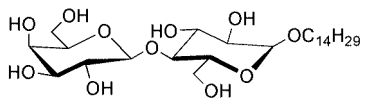

2 Cr 183 SmA 246°C Iso Liq

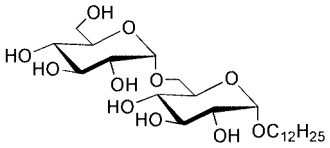

3 Cr 75 Cub 162°C Iso Liq

Fig. 2 Some mesogenic glycolipids derived from disaccharides.[7,8]

such as maltose and lactose;[4–6] see Fig. 2. Dodecyl β-D-maltoside (**1**) and tetradecyl β-D-lactoside (**2**) were each found to exhibit a bilayer smectic A^*_d phase.[7]

n-Dodecyl α-gentiobioside **3**, on the other hand, was found to exhibit a cubic phase.[8] The position of both the alkyl chain and the linkage between the two sugar units engenders a non-linear molecular structure. Therefore, in this case the material self-organises to give a cubic phase where curvature of the layers is present.

Based on the results obtained for the gentiobioside, we chose to move a dodecyl aliphatic chain sequentially from one position to the next in the mono-*O*-(2-hydroxydodecyl)sucrose family of materials, see Fig. 3, and to examine the liquid crystal behaviours of the materials prepared. Sucrose itself provides a unique opportunity to study the combination of a pyranose and a furanose ring system. We have already examined and compared furanose and pyranose based glycolipids which have a single sugar unit in the head group and found that the clearing points of the α and β anomers have an inverted relationship with respect to the ring type of the sugar moiety.[9]

2. Experimental

2.1 Synthesis of materials

The series of sucrose derivatives (**4a–g**) were synthesised as follows:[10,11] sucrose (56 g, 0.16 mol), 1,2-epoxydodecane (purity 96%, Aldrich; 7.4 g, 0.04 mol) and ground potassium hydroxide (2.3 g, 0.04 mol) were added to DMSO (100 ml), and the resultant mixture was heated to 110 °C for 4 h. The mixture was allowed to cool to room temperature and conc. hydrochloric acid was added until the mixture was neutral (pH 7). The mixture was subjected to flash chromatography over silica

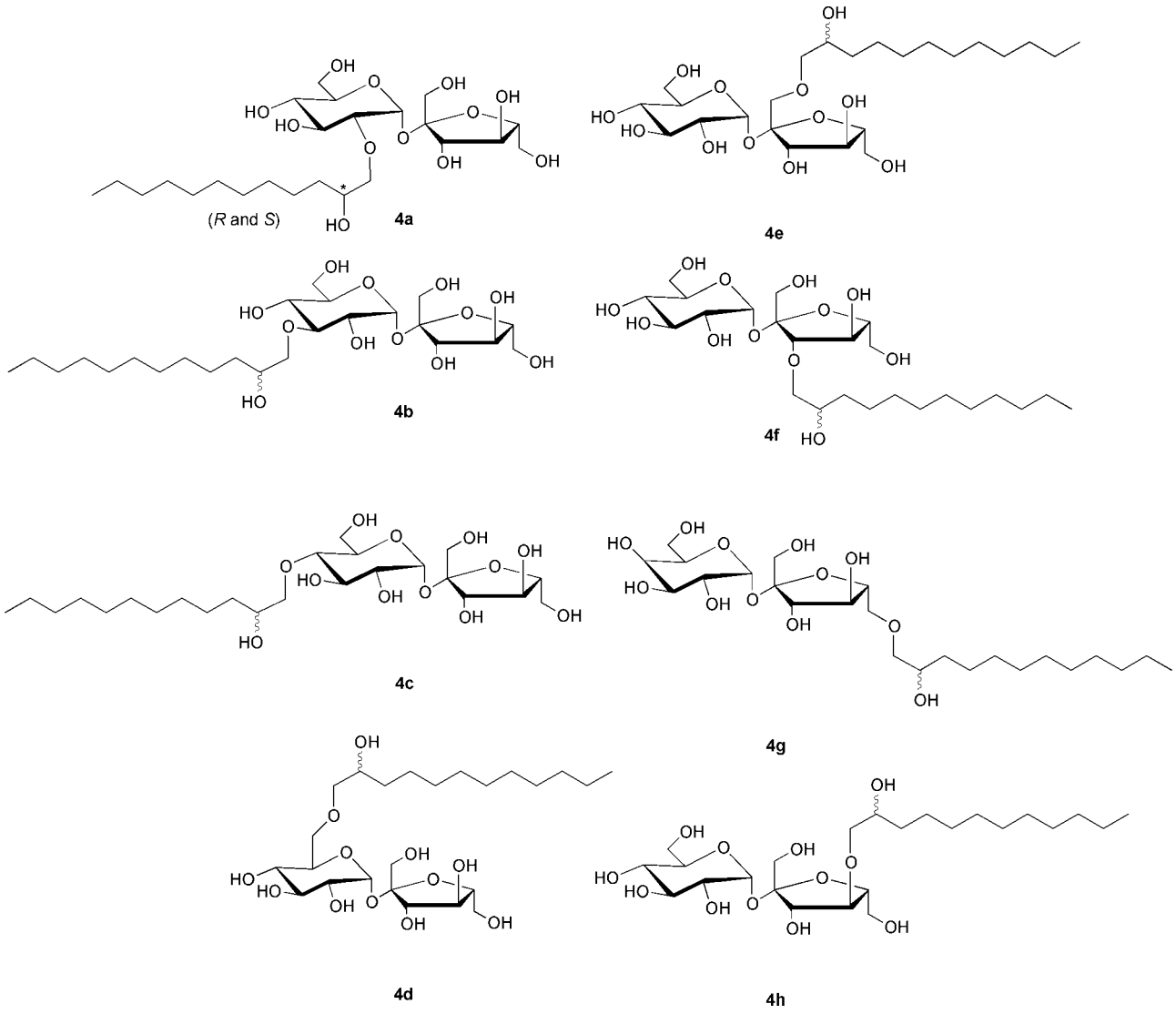

Fig. 3 Target materials, **4a–g**.[10,11]

gel using dichloromethane as the eluent. The first elution volume of dichloromethane was used to remove DMSO and then, elution of the sucrose esters was achieved by the progressive addition of a solvent mixture [CH_2Cl_2–$(CH_3)_2CO$–CH_3OH–H_2O 56 : 20 : 20 : 4] of stronger polarity (R_f monoethers = 0.3–0.4; R_f diethers and dodecane-1,2-diol = 0.6–0.7). This procedure was repeated to remove all diethers and DMSO.

Separation of the regioisomers of the monoesters was made first using preparative HPLC (Nucleoprep NH_2 column, 100 Å, 12 μm, l = 25 cm, id = 40 mm, CH_3CN/H_2O 90/10, 80 ml min^{-1}). The retention times (min) and area (%) for the regioisomers were as follows: **4b** (11.1, 1.5%); **4c** (13.6, 5.5%); **4f** (15.0, 11%); [**4a**(i) (15.8, 17%) and **4a**(ii) (16.8, 17.5%) where (i) and (ii) are epimers]; **4h** (18.3, 8%); **4d** (19.2, 8.5%); **4e** (21.7, 22%); and **4g** (25.2, 9%). The separation was repeated 5 times with samples of approximately 500 mg each in 5 ml of eluent. Further purification of each regioisomer was achieved *via* the use of a more selective semi-preparative column on samples of 200 mg in 2 ml of eluent (Nucleosil column NH_2 100 Å, 5 μm, l = 25 cm, id = 20 mm, eluent CH_3CN–H_2O 88 : 12, 20 ml min^{-1}). The retention times were found to be between 10 and 22 min.

The purity of each product was then checked using analytical HPLC (Nucleosil column NH_2 5 Å, 5 μm, l = 25 cm, id = 4.6 mm, eluent CH_3CN–H_2O 90 : 10, 0.8 ml min^{-1}). Retention times were between 11 and 21 min. Structural evaluations were made *via* the use of ^1H and ^{13}C (D_2O) NMR spectroscopy. The pure samples were lyophilised in order to obtain samples with minimum water content. All of the regioisomers were found to be mixtures of the two epimers generated by the opening of the racemic 1,2-epoxydodecane, except for **4a** for which the separation of the two epimers was possible by HPLC [**4a**(i) and **4a**(ii)] (it should be noted that in the physical studies the racemic mixture was used so that the results obtained would be directly comparable with those obtained for the other materials). The final quantities (mg) of the pure materials were as follows; **4b** (8); **4c** (18); **4f** (61); **4a**(i) (70); **4a**(ii) (98); **4h** (0); **4d** (30); **4e** (98); **4g** (60). The NMR analysis indicated that the **4c** isomer contained very small traces of the **4a** isomers, and that the **4a**(ii) isomer contained very small traces of the **4h** isomer. The **4h** isomer was only obtained in very small quantities, and as it eluted just after a major peak it could not be isolated pure, as a consequence it was not possible to subject this compound to physical testing.

Full analytical data for the regioisomers have been reported previously.[10] Analysis of the NMR spectra gave clear and unambiguous identification of the regioisomers, and elemental analyses were found to be within acceptable limits. However trace amounts of water being present in the materials could not be totally excluded. Nevertheless, experience shows that freeze-drying is the best way to obtain samples with the lowest amount of water present. For mixtures of the regioisomers, which were easily isolated in sufficient quantities to allow for titration using the Karl–Fisher method, a maximum water content of about 2% was obtained. Careful transfer of the samples after freeze-drying was made in order to avoid further up-take of atmospheric moisture due to the hygroscopic nature of the materials.

2.2 Characterisation of the liquid crystalline properties of the materials

Phase identifications and phase transition temperatures were determined by thermal polarised light microscopy using a Zeiss Universal polarizing transmitted light microscope equipped with a Mettler FP82 microfurnace in conjunction with an FP80 Central Processor. Homeotropic sample preparations suitable for phase characterisation were prepared by using clean glass microscope slides (washed with water, acetone, water, concentrated nitric acid, water and dry acetone), whereas homogeneous defect textures were obtained by not using specially cleaned slides.

Phase transition temperatures were determined by differential scanning calorimetry (DSC) using a Perkin Elmer DSC 7-Series with Unix DSC data acquisition and analysis software at a scan rate of 10 °C min^{-1}. The instrument was calibrated against pure indium metal (mp = 156.6 °C, ΔH = 28.5 J g^{-1}).[12] Phase transition temperatures were recorded as the endothermic onset temperature from differential scanning calorimetry traces.

Classification of the mesophases of the products was achieved *via* binary phase diagrams which were constructed by determining the phase transition temperatures of individual binary mixtures of each test material mixed with the standardised compound octyl β-D-glucopyranoside.[13] The binary mixtures were produced by weighing out each individual test material and the known standard material on a microscope slide, and mixing them thoroughly together while in their liquid states. The cooled samples were introduced into the microscope microfurnace and the phase transition temperatures and classification of phase type were performed in the usual manner.

Molecular modelling studies were performed on a Silicon Graphics workstation (Indigo XS24, 4000) using the programs Quanta and CHARMm. Within CHARMm, the Adopted Basis Newton Raphson (ABNR) algorithm was used to locate the molecular conformation with the lowest potential energy. The minimisation calculations were performed until the root mean square (RMS) force reached 4.184 kJ mol^{-1} $Å^{-1}$, which is close to the resolution limit. The RMS force is a direct measure of the tolerance applied to the energy gradient (*i.e.*, the rate of change of potential energy with step number) during each cycle of minimisation. The calculation was terminated in cases where the average energy gradient was less than the specified value. The results of the molecular mechanics calculations were generated using the programs QUANTA V4.0 and CHARMm V22.2. The programs were developed and integrated by Molecular Simulations Inc. The modelling packages assume the molecules to be a collection of hard particles held together by elastic forces, in the gas phase, at absolute zero, in an ideal motionless state, and the force fields used are those described in CHARMm V22.2.

3. Results

3.1 Transition temperatures

The thermotropic liquid crystal properties of the mono-*O*-(2-hydroxydodecyl)sucrose compounds (**4a–g**) were determined by thermal polarised microscopy, the results of which are given in Table 1. The exact melting temperatures of the materials were very difficult to determine because the paramorphotic defect texture of the crystal was retained for a number of degrees into the liquid crystal phase and thus no clearly defined point for the transition from the solid state to the liquid crystal

Table 1 Transition temperatures and phase classification (°C) for the mono-*O*-(2-hydroxydodecyl)sucroses (**4a–g**). Values determined using polarised light thermal microscopy (POM), and where possible, without decomposition, confirmed by DSC

	Cryst		SmA_d*		Cub		Col		Iso Liq
4a	•	132		—	•	135.9	•	147	•
4b	•	125	•	176.5		—		—	•
4c	•	125	•	167.3		—		—	•
4d	•	134	•	186.9		—		—	•
4e	•	154	•	171.1		—		—	•
4f	•	125		—		—	•	147.3	•
4g	•	174	•	190.7		—		—	•

phase could be identified. Consequently, the materials appeared to change from a solid to a soft crystal and only then to the liquid crystal state.

Typically, transition temperatures observed through the microscope are confirmed through the use of differential scanning calorimetry (DSC). In the case of compounds **4a–g**, decomposition or loss of moisture near to the clearing point meant that the DSC data was inconclusive, with the scans consisting of an array of peaks. However, there are a number of trends in melting behaviour that can be drawn from the results presented in Table 1. For instance, the compounds which exhibit lamellar phases (**4b–e** and **4g**) are found to have higher clearing points than the other homologues which exhibit columnar or cubic phases. When the chain is in the position 6 of either the pyranose (**4d**) or furanose ring (**4g**) the liquid crystal to isotropic liquid transition temperature is at its highest; with compound **4d** having the largest temperature range for the mesomorphic state. As the chain is sequentially moved round the disaccharide head group, the clearing points adopt an odd–even effect. Compounds **4a** and **4f** have much lower clearing point temperatures compared to the other members of the series. The different types of mesophases (cubic and columnar) displayed by these materials may be responsible for the reduction in stability.

3.2 Classification of the liquid crystal phases by polarizing light microscopy

Compounds **4b–e** and **4g** were found to exhibit a smectic phase. For all of these compounds, upon cooling from the isotropic liquid, a liquid crystal phase separates in the form of *bâtonnets* which coalesce in the bulk to form focal-conic domains. As the sample is cooled further, the focal-conic domains, which exhibit characteristic elliptical and hyperbolic lines of optical discontinuity,[14] adhere to the surfaces of the glass slides and the resultant texture becomes, in the main part, homeotropic and optically extinct indicating that the phase is optically uniaxial. Due to the strong curvature experienced by the specimens at the edges of defects, such as air bubbles and at the edges of the preparation, focal-conic defects still remain, as shown in Fig. 4 for compound **4d**. The presence of both homeotropic and focal-conic textures together indicates that the mesophase is smectic A in type, which is to be expected for a glycolipid that has a rod-like molecular architecture.

The identification of the smectic A phases of compounds **4b–e** and **4g** was confirmed by miscibility tests using the standard material 1-*O*-octyl β-D-glucopyranoside which is known to exhibit a bilayer smectic A_d* phase. Miscibility across the whole phase diagram was achieved in each case.

Two of the sucrose derivatives were also found to exhibit columnar rather than lamellar liquid crystal phases. Compounds **4a** and **4f** exhibit fan-like defect textures, as shown in Fig. 5. The texture shown in Fig. 5 is characteristic of the presence of a hexagonal columnar phase where the molecules are arranged in a disordered way along the columnar axes. It should be noted that in this photomicrograph no elliptical or hyperbolic lines of optical discontinuity are present as would be expected if the phase were lamellar rather than hexagonal. Although the defect texture is typical of those formed by hexagonal disordered phases, Col_{hd}, X-ray diffraction studies are still required in order to determine that the arrangement of the columns is hexagonal rather than rectangular, and also to determine the organisation of the molecules within the columns.

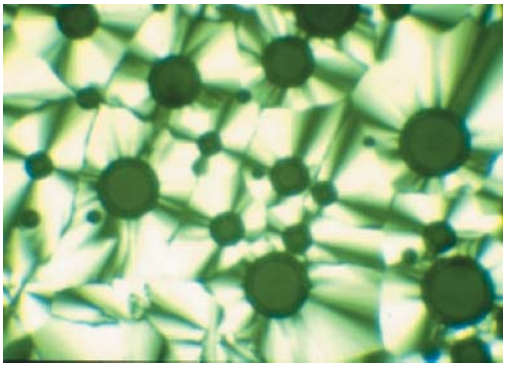

Fig. 5 The fan-like texture of the columnar phase of compound **4a** ($\times 100$). No elliptical or hyperbolic lines of discontinuity are found.

In addition to the formation of a hexagonal phase, compound **4a** was found to exhibit a cubic phase. Although this phase exhibits an optically extinct defect texture, it can be distinguished from a liquid by its high viscosity. The transition on cooling from columnar phase to the isotropic cubic phase is shown in the photomicrograph in Fig. 6 for compound **4a**. The cubic phase can be clearly seen growing in the upper and lower right hand corners of the picture. The fact that this phase is formed at a lower temperature suggests that it is a bicontinuous cubic phase (V_1) rather than a discontinuous mesophase which might be expected to occur at higher temperatures.

3.3 Molecular modelling

In order to comprehend the formation of columnar and cubic phases we probed the gross molecular shapes of the homologous series of materials *via* the use of molecular simulations in the gas phase at absolute zero. It should be noted that this study should only be considered as illustrative as the molecules in the liquid crystal state are undergoing rapid and diffuse reorientational motion. Fig. 7 shows the computer simulations for the sucrose derivatives (**4a–g**). The minimised structures show how the cross-sectional area of the carbohydrate head group changes with respect to that of the aliphatic chain as the chain is moved sequentially from one position to the next. The

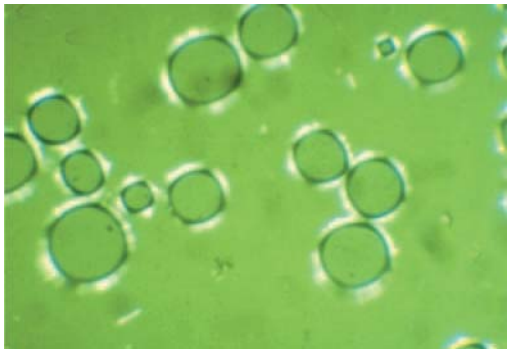

Fig. 4 The homeotropic texture of the smectic A phase of **4d**, showing air bubbles and focal-conic domains ($\times 100$). The polarizers are not crossed at 90° so that the texture becomes visible.

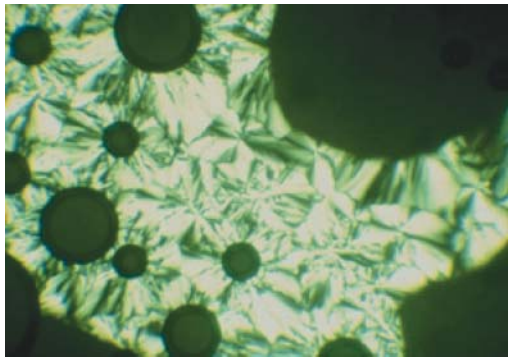

Fig. 6 The transition from the fan-like defect texture of the columnar phase to the isotropic cubic phase (top and bottom right hand corners) for compound **4a** ($\times 100$).

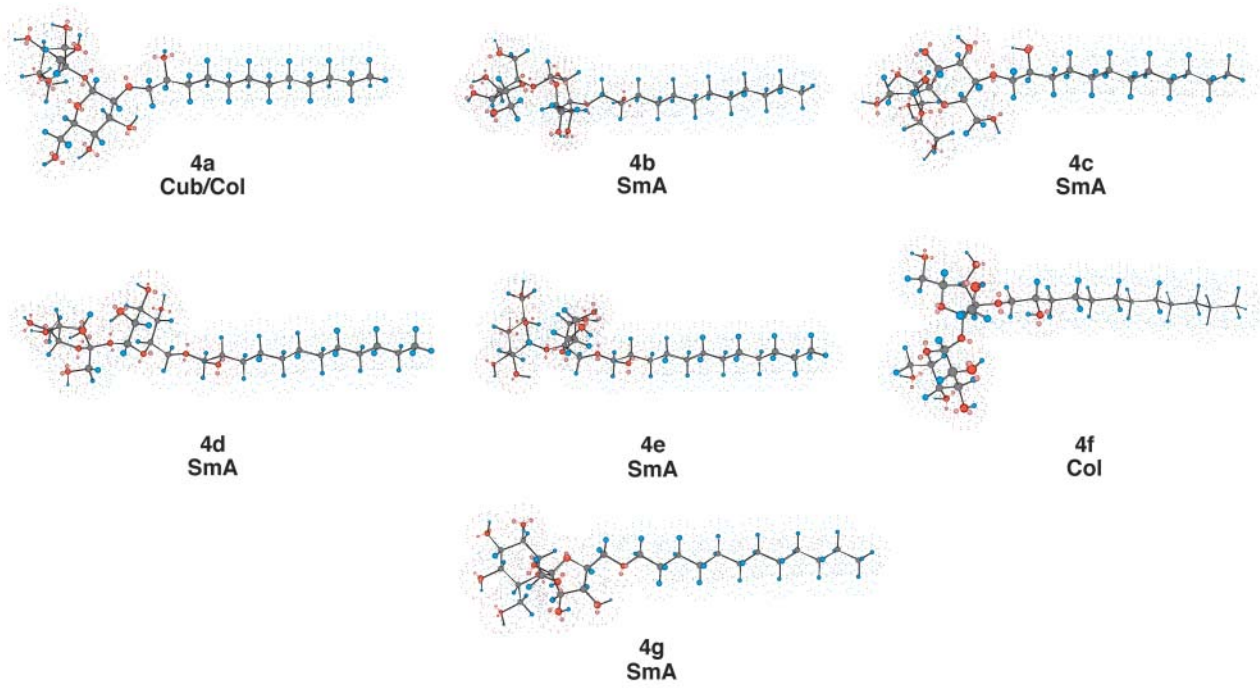

Fig. 7 Computer simulations of compounds **4a–g** showing minimised structures.

molecules that are found to exhibit a smectic phase (**4b–e** and **4g**) adopt a near linear geometry and are therefore expected to self-organise to give a lamellar arrangement of the molecules, *i.e.* little curvature is introduced into the system by the packing together of the molecules. The non-smectic compounds (**4a** and **4f**) appear to have head groups that have larger cross-sectional areas relative to the aliphatic chains due to the location of the point of attachment of the chain itself. Thus, the molecules have wedge-like rather than rod-like gross molecular shapes. The packing of these molecules together, and the extent to which dynamic intermolecular hydrogen-bonding is present, probably leads to curvature being introduced into the local organisation of the molecules. The curvature that is introduced thus appears sufficient to support the formation of cubic and columnar liquid crystal phases.

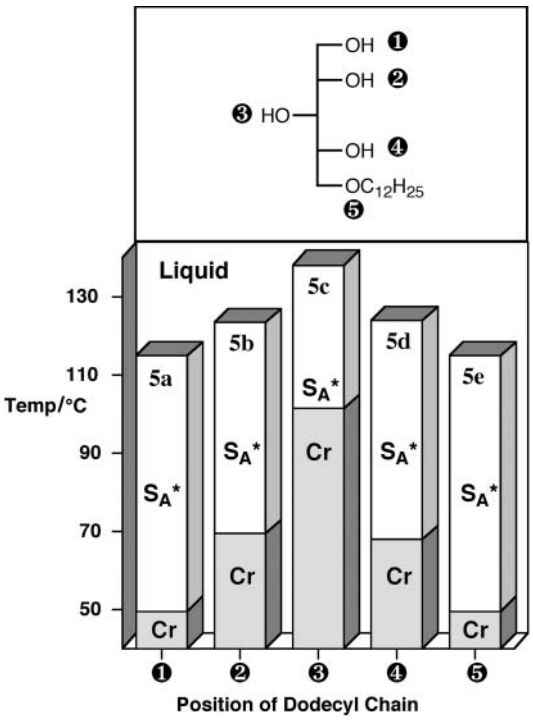

Fig. 8 The effect of chain location on transition temperatures (°C) and mesophase type for the *x*-*O*-dodecyl-D-xylitols, **5a–d**.

4. Discussion

The results demonstrate that the position of attachment of a long aliphatic chain to a sucrose unit result in liquid-crystalline materials being obtained which exhibit a variety of mesophases that are dependent on molecular shape. Previous studies on the *x*-*O*-dodecyl α,β-D-glucopyranoses by Miethchen *et al.*[3] demonstrated the effect on clearing point temperatures as a dodecyl chain is moved sequentially from one position to the next in substituted D-glucopyranose systems, as shown in Fig. 1. However, even though the anomeric concentration ratios for some of the materials varied, the mesophase type exhibited by these systems did not change.

A similar study has also been reported for the acyclic *x*-*O*-dodecyl-D-xylitols **5a–d**.[15] Again all of the homologues in this series were found only to exhibit a smectic A(A*) phase. The results concerning the effect of chain location on the transition temperatures and phase type, see Fig. 8, demonstrate that as the chain is moved to the centre of the carbohydrate moiety, the clearing transition temperatures rise almost linearly with position of attachment, which is due to the increased rigidity of the system which is also reflected in the higher melting points.

Therefore it is clear that the position of substitution of an aliphatic chain in glycolipid systems has a strong effect on transition temperatures, particularly the clearing point. Indeed, there are some indications that accompanying effects associated with molecular flexibility also influence mesophase stability. In the present study, it appears that as the relative size of the head group is increased with respect to the cross-sectional area of the aliphatic chain through change in the position of attachment, then the relative stabilities of the various mesophase types also change. The introduction of curvature by changing the relative cross-sectional areas of the head groups thus plays a similar role to hydration of the head groups in lyotropic systems. Thus the stabilities of the thermotropic phases are similarly susceptible to the inherent curvature introduced into the system by the local molecular

packing as lyotropic phases are to changing solvent concentration. Consequently the thermotropic and lyotropic liquid crystals behave in similar ways with respect to molecular shape and flexibility and induced curvature through the local packing of the molecules.

5. Conclusion

We have demonstrated for glycolipids, that the position of attachment of an aliphatic chain to a disaccharide unit can markedly affect the self-organising properties and structure and bonding features of the material. The location of the attachment can introduce curvature into the system thereby stabilising certain structures over others. The results obtained for the thermotropic liquid crystalline properties of the mono-*O*-(2-hydroxydodecyl)sucroses show a similar dependency on molecular shape and curvature as those found in general for lyotropic systems.

Acknowledgements

The authors would like to thank the CNRS, Béghin-Say and the EPSRC for financial support.

References

1 See for example: D. Demus, H. Demus and H. Zaschke, in *Flüssige Kristalle in Tabellen*, VEB Deutscher Verlag für Grundstoffindustrie, Leipzig, Vol. 1, 1974; D. Demus and H. Zaschke, in *Flüssige Kristalle in Tabellen*, VEB Deutscher Verlag für Grundstoffindustrie, Leipzig, Vol. 2, 1984; G. W. Gray, in *Liquid Crystals and Plastic Crystals*, eds. G. W. Gray and P. A.Winsor, Ellis Horwood, London, Vol. 1, pp. 103–152, 1974.

2 See for example: D. Blunk, K. Praefcke and V. Vill, in *The Handbook of Liquid Crystals, High Molecular Weight Liquid Crystals*, eds. D. Demus, J. W. Goodby, G. W. Gray, H.-W. Spiess and V. Vill, Wiley-VCH, Weinheim, 1998, Vol. 3, Ch. VI, pp. 305–340, and references therein.

3 H. Prade, R. Miethchen and V. Vill, *J. Prakt. Chem.*, 1995, **337**, 427; J. W. Goodby, *Mol. Cryst. Liq. Cryst.*, 1984, **110**, 205; E. Barrall, B. Grant, M. Oxsen, E. T. Samulski, P. C. Moews, J. R. Knox, R. R. Gaskill and J. L. Haberfeld, *Org. Coat. Plast. Chem.*, 1979, **40**, 67; R. Miethchen, J. Holz, H. Prade and A. Lipták, *Tetrahedron*, 1992, **48**, 3061; V. Vill, T. Böcker, J. Thiem and F. Fischer, *Liq. Cryst.*, 1989, **6**, 349.

4 B. Pfannemuller, W. Welte, E. Chin and J. W. Goodby, *Liq. Cryst.*, 1986, **1**, 357.

5 V. Vill, T. Bocker, J. Thiem and F. Fischer, *Liq. Cryst.*, 1989, **6**, 349.

6 Y. D. Ma, A. Takada, M. Sugiura, A. Fukuda, T. Miyamoto and J. Watanabe, *Bull. Chem. Jpn.*, 1994, **67**, 346.

7 M. A. Marcus, *Mol. Cryst. Liq. Cryst. Lett. Sect.*, 1986, **3**, 85.

8 S. Fischer, H. Fischer, S. Diele, G. Pelzl, K. Jankowski, R. R. Schmidt and V. Vill, *Liq. Cryst.*, 1994, **17**, 855.

9 J. W. Goodby, J. A. Haley, G. Mackenzie, M. J. Watson, V. Ferrieres and D. Plusquellec, *J. Mater. Chem.*, 1995, **5**, 2209.

10 J. Gagnaire, G. Toraman, G. Descotes, A. Bouchu and Y. Queneau, *Tetrahedron Lett.*, 1999, **40**, 2757.

11 J. Gagnaire, A. Cornet, A. Bouchu, G. Descotes and Y. Queneau, *Colloids Surf.*, 2000, **172**, 125.

12 CRC Handbook of Physics and Chemistry, ed. R. C. Priest, CRC Press, Boca Raton, 68th Edition, 1988.

13 J. W. Goodby, *Mol. Cryst. Liq. Cryst.*, 1984, **110**, 205; E. Barrall, B. Grant, M. Oxsen, E. T. Samulski, P. C. Moews, J. R. Knox, R. R. Gaskill and J. L. Haberfeld, *Org. Coat. Plast. Chem.*, 1979, **40**, 67.

14 G. W. Gray and J. W. Goodby, in *Smectic Liquid Crystals: Textures and Structures*, Leonard Hill, Philadelphia, 1984.

15 J. W. Goodby, J. A. Haley, M. J. Watson, G. Mackenzie, S. M. Kelly, P. Letellier, P. Godé, G. Goethals, G. Ronco, B. Harmouch, P. Martin and P. Villa, *Liq. Cryst.*, 1997, **22**, 497.